

PAPER • OPEN ACCESS

Statistical evaluation of damage size based on amplitude mapping of damage-induced ultrasonic wavefield

To cite this article: Chia Sheng Gan *et al* 2018 *IOP Conf. Ser.: Mater. Sci. Eng.* **405** 012006

View the [article online](#) for updates and enhancements.

You may also like

- [Investigation of the damage effect on electromagnetic performance evaluation of a radar absorbing structure](#)
Jong-Min Hyun, Seung-Chan Hong and Jung-Ryul Lee
- [Damage size characterization algorithm for active structural health monitoring using the \$A_0\$ mode of Lamb waves](#)
Rahim Gorgin, Zhanjun Wu, Dongyue Gao et al.
- [A multi-level damage classification technique of aircraft plate structures using Lamb wave-based deep transfer learning network](#)
Wei-han Shao, Hu Sun, Yishou Wang et al.



ECS
The
Electrochemical
Society
Advancing solid state &
electrochemical science & technology

DISCOVER
how sustainability
intersects with
electrochemistry & solid
state science research

Statistical evaluation of damage size based on amplitude mapping of damage-induced ultrasonic wavefield

GAN Chia Sheng ¹, CHIA Chen Ciang ^{1,*}, TAN Lin Yaw ¹, Norkhairunnisa MAZLAN ¹, Joel B. HARLEY ²

¹ Dept. of Aerospace Engineering, Universiti Putra Malaysia, Selangor, Malaysia

² Dept. of Electrical and Computer Engineering, University of Florida, Florida, USA

* chia_cc@upm.edu.my

Abstract. The inability to statistically evaluate the damage size based on amplitude mapping has long plagued the ultrasound propagation imaging (UPI) system and related non-destructive evaluation (NDE) community. This paper proposes a damage visualization method called the Statistically Thresholded Anomaly Mapping (STAM) method to solve this problem. It could isolate the damage-induced anomalous waves from an ultrasonic full wavefield data, map their amplitudes into an image and statistically differentiate damage from the background noise and pristine region of a specimen, without prior knowledge or reference data of the specimen being inspected. The proposed method was demonstrated through the visualization and evaluation of a thermal damage inflicted in a glass fibre reinforced composite specimen. The effects of two parameters on result quality and accuracy of damage size evaluation were studied by varying their values independently. The optimized result showed that 99.9% of the background noises could be removed while maintaining clear visualization of damage, hence allowing the users to evaluate the presence, location, shape, size and severity of the damage accurately.

1. Introduction

Ultrasounds are widely used in the material and structural nondestructive evaluation (NDE) due to its sensitivity towards physical properties such as volume, thickness, temperature and most importantly, damages or anomalies that are present on the surface or within the material [1]. In order to harvest these information that ultrasounds carry, the ultrasound propagation imaging (UPI) system had been developed [2] for NDE of plate-like waveguides such as aircraft wings [3] and radome panels [4]. UPI system and its associated result processing methods had shown the capabilities of revealing damages such as small cracks through the detection of anomalous waves, which corresponds to the scattering and reflected waves when an ultrasonic wave encounters a damage [5,6]. In recent years, UPI system had been further improved to give higher visibility to these anomalous waves. The result processing methods, which suppress incident waves through the subtraction of adjacent waves [5], frequency-wavenumber domain filtering [7,8] and model-driven wavefield baseline subtraction [9], proved that the suppression of incident waves reveals anomalous waves clearly, thus revealing the presence and location of damage.

However, these methods do not have statistical reliability when it comes to damage sizing and the results are typically in the video forms where the inspectors have to estimate the size of a damage by repeatedly examining the result videos, which is both unreliable and also inaccurate. This becomes a significant problem when the damage is incorrectly evaluated and its severity is underestimated. For



Content from this work may be used under the terms of the [Creative Commons Attribution 3.0 licence](https://creativecommons.org/licenses/by/3.0/). Any further distribution of this work must maintain attribution to the author(s) and the title of the work, journal citation and DOI.

example, aircrafts are likely to get struck by lightning once every 10,000 hours of flight on average [10], which for an aircraft that is built mostly of composites such as Boeing 787, it is highly hazardous to underestimate the inevitable lightning damage as the lightning damages can severely degrade the mechanical properties of composites [11, 12]. Tragedies involving the loss of countless lives might occur if the composites' damages deteriorate its mechanical strength to a critical level and causes a failure mid-flight. Therefore, it is of utmost importance to have statistical reliability when it comes to the detection and evaluation of damages.

Previously, Capriotti et al. (2017) used Multivariate Outlier Analysis (MOA) to statistically analyse ultrasonic signals in comparison to an ultrasonic signal obtained from a pristine region of the same specimen [13]. Through the use of the Mahalanobis Squared Distance as part of the MOA, a Damage Index (DI) was obtained, whereby a large value of DI represents a damage. In their paper, MOA is reported to have 100% probability of detection while having a 10% probably of false alarms. Although this method has a high probability of detection, there exists an uncertainty of whether the pristine region of specimen used to obtain the reference signal is truly free from manufacturing defects. If such pristine region indeed exists, then paradoxically, its location must be known prior to the processing of inspection data. Other than that, the outcome of the analysis is unable to determine the sizes of the damages, which is a crucial information in order to evaluate the severity of any damage.

To solve the inability of obtaining a statistically reliable result, this paper describes a reference-free method that provides a statistical damage threshold to the results obtained from amplitude mapping of the damage-induced ultrasonic wavefield, where values higher than the threshold are considered as a damage. Through the use of the threshold, the amplitude map will be rid of noises, leaving an amplitude map that shows only the damages. This method allows the damage sizes to have an absolute value instead of undesirable and indecisive estimations by examining the result videos repeatedly.

2. The proposed method

The proposed method is called Statistically Thresholded Anomaly Mapping (STAM). It is suitable for processing of any ultrasonic full wavefield data acquired using UPI system, regardless if the ultrasonic excitation-sensing is achieved using a scanning laser exciter and a fixed piezoelectric sensor, or a fixed piezoelectric exciter and a scanning laser Doppler vibrometer (LDV) sensor. This method has an anomalous waves isolation component and a damage threshold calculation component, described in the following sections.

2.1. Anomalous waves isolation

Due to the dispersive nature of ultrasound, waves guided by plate-like waveguides often have multiple modes mixed or overlapped in time [14, 15]. Wave modes which exist due to inspection excitation are collectively known as the incident modes. When these incident modes reflected by the damages have insufficient propagation time to separate from each other near damages, mode conversion occurs [16]. These mode-converted waves, also known as the anomalous waves, typically have a magnitude of a few orders smaller than the incident ones. Their small magnitude and the mix-modal characteristics make them unnoticeable at all or hard to be noticed, hence making the detection of damage associated with these anomalous waves difficult.

In order to isolate the anomalous waves, the acquired ultrasonic wavefield signals are first grouped together as a three-dimensional (3D) spatiotemporal data matrix. After that, the 3D data undergoes a 3D DFT (discrete Fourier transform) to transform from the space-time domain to the wavenumber-frequency domain [17–19]. Once transformed, the incident modes are usually demixed and easily distinguishable in the wavenumber-frequency domain. They are then suppressed or filtered out using a mode filter described in [19]. For thin plate-like materials typically used in the aerospace structural applications, the maximum number of modes exists is usually two, hence only one step of filtering is needed. As long as the wavenumber and the frequency of the anomalous waves are different from the incident modes, the anomalous waves will remain in the mode-filtered data, hence isolated for further processing.

The process of rendering the anomalous waves into an amplitude map to show the presence and location of damages can be done by determining the peak-to-peak amplitudes of all mode-filtered signals and mapping the values into an intensity graph while conserving their relative spatial position. By using suitable colour scale, a stark contrast between the damage and pristine areas can be realized, which allows one to easily identify the damaged areas from the pristine areas. This is because after the removal of incident modes, only the anomalous waves and noises remain in the 3D data matrix, with damaged areas containing the anomalous waves and the pristine areas containing the noises. These anomalous waves' amplitudes are higher than the noise floor. When a suitable colour scale is used, the damages can be easily identified. A suitable variable time window, as described in [5], such as where the peak-to-peak amplitude of anomalous waves are at the highest and the noise at the lowest, can also be used optionally to increase the contrast between the peak-to-peak amplitudes of anomalous waves and noises so that the clearest result can be produced. This anomalous waves isolation method offers the advantage of not being dependent on correct selection of any wave mode for damage evaluation, hence circumvented the need of performing reference inspection of the specimen at pristine state to understand the complex ultrasonic waves and modes.

2.2. Damage threshold calculation

To distinguish damages from background noises in an amplitude map, a statistical damage threshold is proposed. The damage threshold (DT) is defined as in Eqn. 1, where μ and σ represents the mean and standard deviation of background noises, respectively, while M represents a constant multiplier.

$$DT = \mu + M\sigma, \quad (1)$$

To determine μ , each pixel value is first ranked from the lowest value to the highest value. After that, the sum of values starting from the lowest rank up to the N^{th} rank is divided by N . The amplitude map is then masked according to Eqn. 2, where $V(x, y)$ represents the value of a pixel at location (x, y) .

$$V(x, y) = \begin{cases} 0, & V(x, y) \leq DT \\ V(x, y), & V(x, y) > DT \end{cases}, \quad (2)$$

The final output is an amplitude map devoid of noises such that the damages can be visualized, and their sizes and also locations can be accurately determined. The damage threshold is suitable for any anomalous waves amplitude map as long as the N number of pixels do not contain anomalous wave values.

3. Experimental validation

3.1. Acquisition of ultrasonic wavefield data

An ultrasonic full wavefield data matrix was acquired using an Ultrasound Propagation Imaging (UPI) system [2]. The system consists of a custom-made diode-pumped solid-state Nd:YAG (neodymium-doped yttrium aluminium garnet) pulsed laser (PL) as the source for ultrasonic waves on the specimen, a galvano-motorized laser mirror scanner (LMS) to point the laser to the intended impingement grid points, a fixed broadband ultrasound sensor with 350kHz cut-off to detect ultrasonic waves originating from the impingement points, an oscilloscope to digitize the detected waves from the sensor, and a computer for hardware synchronization, data storage, result processing, and result display. The PL has a wavelength of 532nm, a beam diameter of 4mm, a divergence of 0.5mrad and a pulse duration of 30ns, which is capable of producing ultrasonic waves non-destructively at the impingement point due to the transient thermoelastic expansion and contraction phenomenon [3]. The PL fires the laser at the LMS that is specially made to reflect lasers with 532nm wavelengths. The two computer-controlled galvano-motorized mirrors inside the LMS, which stand orthogonally from each other, directs the laser to the intended impingement grid points by rotating the mirrors they are attached to. By controlling the LMS, the laser impinges the area of inspection interest in a raster pattern, starting from the top left corner to the bottom right corner in an x by y grid with the same scan distance intervals for both the x and y axes.

From each laser impingement point, ultrasonic waves propagate and disperse into mixed multimodal ultrasonic waves that are detected by the sensor. The ultrasonic signals are then received by the oscilloscope to be digitized and sent to the computer for storage and processing.

3.2. Specimen

Specimen used in this study was fabricated in-house from a 250 by 250mm glass fibre reinforced epoxy prepreg (HEXCEL, BMS 8-79 Style 1581 with HexPly F155 resin system) as a 1-layer [(0/90)] lamina. Curing was done in vacuum bagging at 74 kPa, heated by thermal blanket at a rate of 4°C/min, followed by 90 minutes dwell at 127°C, and cool down to room temperature at 3°C/min. The thermal damage of the specimen was inflicted by contact heating using a 20mm diameter aluminium rod heated to 1.5 times of T_g (glass transition temperature), i.e. 182°C, for 30 minutes. Inspection scan was conducted on the specimen over an 80 by 80mm area with an interval of 0.5mm in both the x and y axes. Based on origin located at the lower left corner of inspection area, the center of the thermal damage was located at position (47, 35) mm and the sensor located at position (45, -105) mm. The acquired ultrasonic signals were then processed using the Statistically Thresholded Anomaly Mapping (STAM) method.

4. Results and discussion

4.1. Effects of anomalous waves isolation

Figure 1 shows a representation of frequency-wavenumber data in grey-scale, where signals with the highest and lowest amplitude are shown in white and black, respectively. Figure 1(a) clearly shows the incident wave mode as white lines spanning from 0m^{-1} to 200m^{-1} in the wavenumber (K) axis and 0kHz to 350kHz in the frequency (F) axis. It should be noted that the abrupt stop at 350kHz was caused by the sensor's detection range of up to 350kHz. Figure 1(b) shows the frequency-wavenumber (FK) map after filtering out the incident mode through the use of a wavenumber filter with a 37.5m^{-1} half-power taper bandwidth (B_M) and 12.5m^{-1} upper (C_H) and lower (C_L) wavenumber cutoffs, along the white FK lines that represent the incident mode. The filter was designed to radiate from the origin of FK axis to the infinity, suppressing all signals within its effective band to low amplitude, hence the filtered zone appeared as black regions extending to the top of Figure 1(b).

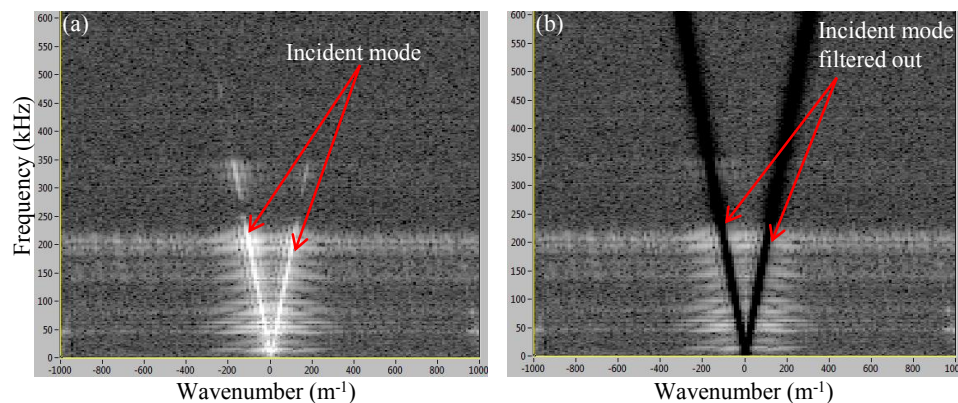


Figure 1. Frequency-wavenumber map (a) before and (b) after filtering of incident wave mode

Figure 2 shows intermediate inspection results after each step of data processing. Photograph of the specimen is given in Figure 2(a). It shows charring within the thermal damage infliction area that is indicated with a dotted circle. A snapshot from the ultrasound wavefield propagation imaging (UWPI) [2] video before and after the filtering of incident mode is given in Figure 2(b) and (c), respectively. The anomalous waves caused by the thermal damage is obscured by high amplitude of incident waves, hence unnoticeable in Figure 2(b). Once the incident mode was filtered out, the anomalous waves can clearly be seen in the middle of Figure 2(c), despite polluted by background noises. Further processing the

mode-filtered data into an amplitude map enhanced the visibility of the damage, as shown in Figure 2(d). Note that the amplitude map facilitates easy detection of the damage, but the size of the damage could not be measured directly since the boundary of the damage could not be clearly defined yet, due to the background noises.

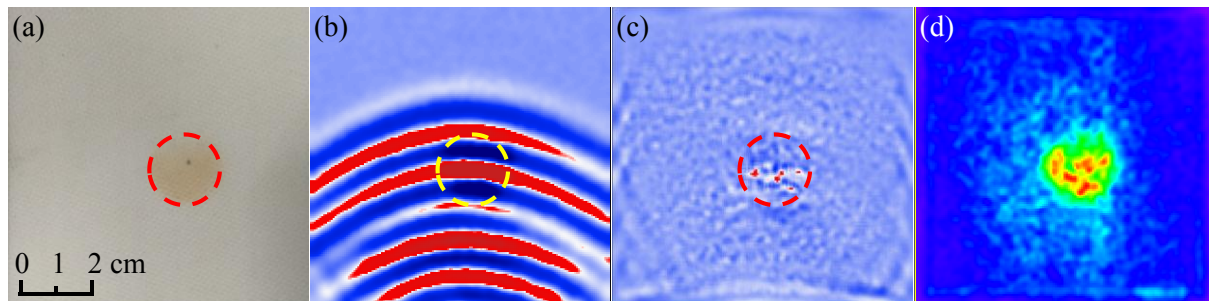


Figure 2. Intermediate inspection results based on (a) naked eye inspection; UWPI video snapshots (b) before and (c) after filtering of incident wave mode; and (d) amplitude map of anomalous waves without damage thresholding.

4.2. Effects of damage thresholding

Statistically Thresholded Anomaly Mapping (STAM) result images will be produced after applying the damage threshold. There are two variables affecting the results. The first variable is the value of N , which physically represents the number of samples used for the calculation of damage threshold. The value of this variable is more conveniently determined as P , which is a percentage of the total pixel number in an amplitude map. Applying the damage threshold calculated based on a constant value of $M = 4$ but varying the value of P from 10% to 50% gives interesting results in Figure 3. When a higher P is used, the background noise in the STAM image is significantly reduced. This is because, as more noise samples are gathered, the mean and standard deviation of background noise are closer to their true values. Reduction of background noises is important to allow the users to be able to distinguish the damaged area from the pristine area without a doubt regarding the actual damage size depicted by the STAM image. Concluding from these results, $P = 50\%$ is preferred as it has the least background noises. Setting P to a value higher than 50% is not preferred as users wouldn't know the damage size beforehand in real life cases, such that it poses a possibility of regarding a damaged area as noise and subsequently remove it from the final result, which in turn causes underestimation of the real damage size.

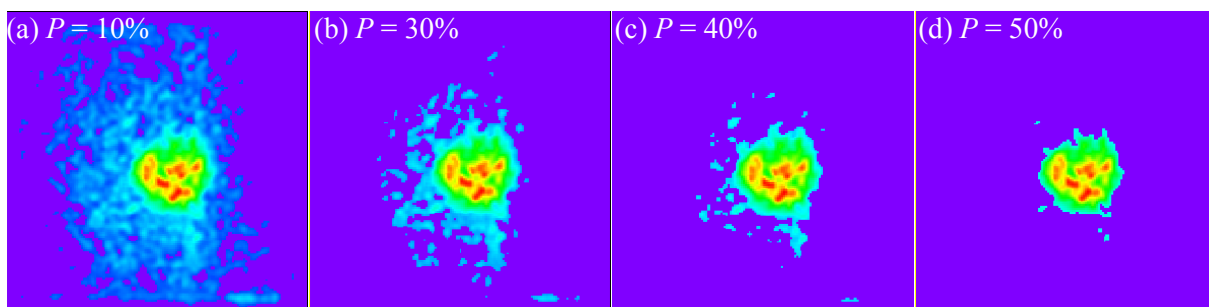


Figure 3. STAM images after applying a damage threshold calculated based on a constant $M = 4$ and different statistical sample size P at (a) 10%, (b) 30%, (c) 40%, and (d) 50%

The second variable affecting the results is the multiplier M in Eqn. 1. STAM images after applying the damage threshold calculated based on a constant value of $P = 50\%$ but varying the value of M from 1 to 8 are given in Figure 4. According to the Empirical Rule, 68% of data, which in this case is the background noise, falls within 1 standard deviation of mean, 95% of data falls within 2 standard deviations of mean and finally, 99.7% of data falls within 3 standard deviations of mean. By using $M = 4$, it is assumed that 99.9% of background noise will be covered, which means that the result will

be noise free with a 99.9% confidence. Since $M = 4$ will result in a 99.9% removal of background noise, it can be concluded that it is the best choice as it is redundant to go higher than that. Other than that, a higher multiplier poses a threat of setting the damage threshold value too high such that even the damaged areas would be classified as background noise. This is shown in the Figure 4(d) where the damage could be measured to have a 20 mm diameter, even when the thermal damage can be safely assumed to be larger than that, simply because heat may be conducted to the surrounding of actual contact area with the 20 mm diameter heat damage inflicting aluminium rod. This proves that when $M = 8$ is used, only the most damaged area will be considered as damage while the less damaged area is considered as noise.

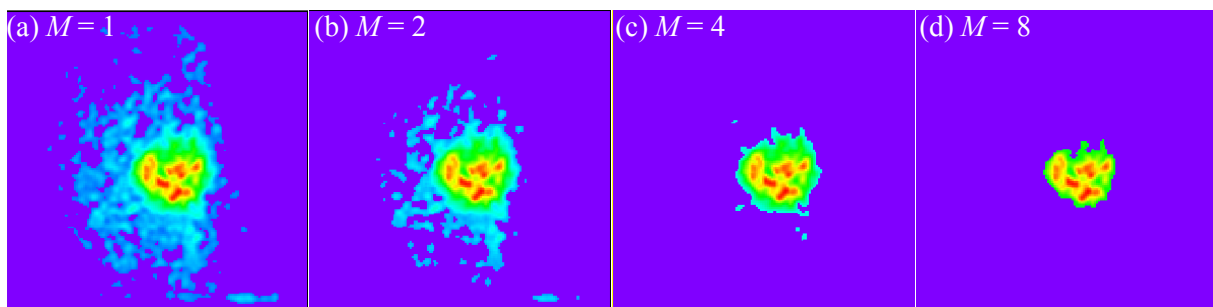


Figure 4. STAM images after applying a damage threshold calculated based on a constant $P = 50\%$ and different values of multiplier when (a) $M = 1$, (b) $M = 2$, (c) $M = 4$, and (d) $M = 8$.

5. Concluding remarks

The inability to statistically evaluate the damage size based on amplitude mapping has long plagued the UPI system. This paper proposed a damage visualization method called the STAM method to solve this problem. The STAM can isolate anomalous waves that are mode-converted from incident waves-damage interaction, and then map their amplitudes into an image in which the existence and location of damages can be visualized. The boundaries of damages can be identified by utilizing the statistical damage threshold calculation component of STAM, which facilitates accurate damage size evaluation.

Experimental validation of the proposed STAM method was conducted by inspecting a glass fibre reinforced polymer specimen inflicted with a thermal damage. A UPI system with scanning laser as ultrasound exciter and a fixed broadband ultrasound sensor was used to acquire the ultrasonic full wavefield data. Intermediate result in the form of anomalous waves amplitude map showed that the thermal damage could be clearly visualized, although the map suffered from some background noises. The effect of the statistical damage threshold calculation component of the STAM was examined by varying two parameters independently, i.e. M , the standard deviation multiplier, and P , the number of samples used for the calculation of damage threshold in term of percentage of total pixel number in the amplitude map. The results showed that $P = 50\%$ and $M = 4$ is the best combination to accurately evaluate the shape and size of the damage while eliminating 99.9% of background noises.

The proposed STAM method proved to be able to accurately locate and determine the size of a damage as long as anomalous waves are present in the ultrasonic wavefield data. It has the advantage of not requiring a reference data from a pristine specimen or a pristine region of the same specimen. Furthermore, its functionality and accuracy are not dependent on the correct selection of any specific wave mode, hence circumvented the need of performing reference inspection or numerical study of pristine specimen for the understanding of the complex ultrasonic waves and modes. The statistical damage threshold calculation component of STAM is suitable for other anomalous waves amplitude mapping applications as well, provided that damaged area is smaller than $P = 50\%$ of imaging area.

The authors are currently improving the STAM method by optimizing the incident mode filter so that even the incident waves at the edges can be filtered out fully. Quantitative accuracy and reliability analysis are also underway.

Acknowledgement

This work was supported by the Universiti Putra Malaysia through research project GP/2017/9564300.

References

- [1] Kouche A E, Hassanein H S. Ultrasonic non-destructive testing (NDT) using wireless sensor networks. *Procedia Comput Sci* 2012; 10:136–43
- [2] Chia C C, Lee J R, Park J S, Yun C Y, Kim J H. New design and algorithm of ultrasound propagation imaging system using Q-switched pulsed laser. 38th Int Conf Defektosk, 2008
- [3] Chia C C, Jeong H-M, Lee J-R, Park G. Composite aircraft debonding visualization by laser ultrasonic scanning excitation and integrated piezoelectric sensing. *Struct Control Heal Monit* 2012; 19: 605–20
- [4] Chia C C, Lee J R, Park C Y. Radome health management based on synthesized impact detection, laser ultrasonic spectral imaging, and wavelet-transformed ultrasonic propagation imaging methods. *Compos Part B Eng* 2012; 43: 2898–906
- [5] Lee J-R, Chia C C, Park C-Y, Jeong H. Laser ultrasonic anomalous wave propagation imaging method with adjacent wave subtraction: Algorithm. *Opt Laser Technol* 2012; 44:1507–15
- [6] Chia C C, Lee J-R, Park C-Y, Jeong H-M. Laser ultrasonic anomalous wave propagation imaging method with adjacent wave subtraction: Application to actual damages in composite wing. *Opt Laser Technol* 2012; 44:428–40
- [7] Michaels T E, Ruzzene M, Michaels J. Incident wave removal through frequency-wavenumber filtering of full wavefield data. *AIP Conf Proc* 2009; 1096: 604–11
- [8] Michaels T E, Ruzzene M, Michaels J E. Frequency-wavenumber domain methods for analysis of incident and scattered guided wave fields. *Heal Monit Struct Biol Syst* 2009; 7295: 729513–729513–12
- [9] Alguri K S, Chia C C, Harley J B. Model-driven, wavefield baseline subtraction for damage visualization using dictionary learning. In: Chang F, Kopsaftopoulos F, editors. *Proc. 11th IWSHM*, vol. 2, Stanford, California, USA: DEStech Publications, Inc; 2017, p. 2276–83
- [10] Larsson A. The interaction between a lightning flash and an aircraft in flight. *Comptes Rendus Phys* 2002; 3:1423–44
- [11] Gagné M, Therriault D. Lightning strike protection of composites. *Prog Aerosp Sci* 2014; 64:1–16
- [12] Hirano Y, Katsumata S, Iwahori Y, Todoroki A. Artificial lightning testing on graphite/epoxy composite laminate. *Compos Part A Appl Sci Manuf* 2010;41: 1461–70
- [13] Capriotti M, Kim H E, Di Scalea F L, Kim H. Detection of major impact damage to composite aerospace structures by ultrasonic guided waves and statistical signal processing. *Procedia Eng* 2017; 199:1550–5
- [14] Lamb H. On waves in an elastic plate. *Proc R Soc London Ser A* 1917; 93:114–28
- [15] Rose J L. *Ultrasonic waves in solid media*. Cambridge, UK: Cambridge University Press; 1999
- [16] Pieczonka Ł, Ambroziński Ł, Staszewski W J, Barnoncel D, Pérès P. Damage detection in composite panels based on mode-converted Lamb waves sensed using 3D laser scanning vibrometer. *Opt Lasers Eng* 2017; 99:80–7
- [17] Ruzzene M. Frequency–wavenumber domain filtering for improved damage visualization. *Smart Mater Struct* 2007; 16:2116–29
- [18] Michaels T E, Michaels J E, Ruzzene M. Frequency-wavenumber domain analysis of guided wavefields. *Ultrasonics* 2011; 51:452–66
- [19] Flynn E B, Chong S Y, Jarmer G J, Lee J-R. Structural imaging through local wavenumber estimation of guided waves. *NDT E Int* 2013; 59:1–10